Development 129, 3693-3704 (2002)
Printed in Great Britain © The Company of Biologists Limited 2002
DEV5032

Two linked *hairy/Enhancer of split*-related zebrafish genes, *her1* and *her7*, function together to refine alternating somite boundaries

Clarissa A. Henry[1,*], Michael K. Urban[1,*], Kariena K. Dill[1], John P. Merlie[1], Michelle F. Page[1], Charles B. Kimmel[2] and Sharon L. Amacher[1,‡]

[1]Department of Molecular and Cell Biology, University of California, Berkeley CA 94720-3200, USA
[2]Institute of Neuroscience, University of Oregon, Eugene, OR 97403-1254, USA

*These authors contributed equally
‡Author for correspondence (e-mail: amacher@uclink4.berkeley.edu)
The authors dedicate this paper to the memory of Loan Thanh Nguyen, our labmate and friend

Accepted 9 May 2002

SUMMARY

The formation of somites, reiterated structures that will give rise to vertebrae and muscles, is thought to be dependent upon a molecular oscillator that may involve the Notch pathway. *hairy/Enhancer of split related* [*E(spl)*]-related (*her* or *hes*) genes, potential targets of Notch signaling, have been implicated as an output of the molecular oscillator. We have isolated a zebrafish deficiency, *b567*, that deletes two linked *her* genes, *her1* and *her7*. Homozygous *b567* mutants have defective somites along the entire embryonic axis. Injection of a combination of *her1* and *her7 (her1+7)* morpholino modified antisense oligonucleotides (MOs) phenocopies the *b567* mutant somitic phenotype, indicating that *her1* and *her7* are necessary for normal somite formation and that defective somitogenesis in *b567* mutant embryos is due to deletion of *her1* and *her7*. Analysis at the cellular level indicates that somites in *her1+7*-deficient embryos are enlarged in the anterior-posterior dimension. Weak somite boundaries are often found within these enlarged somites which are delineated by stronger, but imperfect, boundaries. In addition, the anterior-posterior polarity of these enlarged somites is disorganized. Analysis of *her1* MO-injected embryos and *her7* MO-injected embryos indicates that although these genes have partially redundant functions in most of the trunk region, *her1* is necessary for proper formation of the anteriormost somites and *her7* is necessary for proper formation of somites posterior to somite 11. By following somite development over time, we demonstrate that *her* genes are necessary for the formation of alternating strong somite boundaries. Thus, even though two potential downstream components of Notch signaling are lacking in *her1+7*-deficient embryos, somite boundaries form, but do so with a one and a half to two segment periodicity.

Key words: Paraxial mesoderm, Presomitic mesoderm, Somitogenesis, Notch signaling, *her1*, *her7*, Zebrafish

INTRODUCTION

Segmentation of the body is a feature of development common to many animals. There are at least two modes of segmentation: the division of an existing tissue and the sequential division of a continuously growing tissue. Within the insects, segmentation in long germ band insects involves the division of an existing tissue whereas segmentation in short germ band insects is an example of the latter mode. During vertebrate development, rhombomeres form from an existing field of cells in the hindbrain, but somites form from a continuously proliferating field of cells. As it is not yet clear if the segmentation of long germ band and short germ band insects reflects conserved mechanisms (reviewed by Davis and Patel, 2002), it is an outstanding question as to whether there is any conservation of segmentation strategies between insects and vertebrates.

The anterior to posterior formation of somites from the presomitic mesoderm (PSM) is a highly dynamic process that underlies much of the segmentation of the adult. Many models of somitogenesis propose the existence of oscillatory behavior in the PSM as one method of creating pattern from an equivalent field of cells. In the 'clock and wavefront' model, cells in the PSM cycle between permissive and nonpermissive states (the 'clock') (Cooke and Zeeman, 1976). When this 'clock' interacts with a 'wavefront' (a maturation signal that tells cells to segment), cells in the anterior PSM in the permissive state form a somite. Presumptive somites, as well as formed somites, comprise an anterior compartment and a posterior compartment (Keynes and Stern, 1988) (reviewed by Hirsinger et al., 2000). This has led to the suggestion that a somite boundary may be specified at the juxtaposition of anterior and posterior cell fates (Meinhardt, 1986; Durbin et al., 1998; Durbin et al., 2000). In Meinhardt's model, cells oscillate between anterior and posterior cell fates (Meinhardt, 1986). A single cell expresses one cell fate and instructs neighboring cells to adopt the opposite fate. This gives rise to oscillations in the PSM that generate stable stripes of cells

expressing anterior and posterior fates in the anteriormost PSM. A somite boundary would then form at the juxtaposition of anterior and posterior cells.

One pathway that has been implicated as playing a role in biochemical oscillations that underlie somitogenesis is the Notch signaling pathway. Homozygous null mice for the Notch pathway members *Notch*, *Dll1*, *RBPJk*, *presenilin*, and *Lunatic fringe* all display defects in somite formation (Hrabe de Angelis et al., 1997; Conlon et al., 1995; Oka et al., 1995; Zhang and Gridley, 1998; Evrard et al., 1998; Koizumi et al., 2001). In zebrafish, most of the fused somites class of mutations, including *after eight/deltaD*, that are neurogenic and thought to disrupt the Notch pathway, produce defects in somitogenesis (van Eeden et al., 1996; van Eeden et al., 1998; Holley et al., 2000; Gray et al., 2001).

The most compelling evidence for a molecular oscillator in the PSM was the discovery that a chick homolog of *Drosophila hairy*, called *hairy1*, was expressed in a dynamic pattern (Palmeirim et al., 1997). During somitogenesis, *hairy1* is expressed in successive posterior-to-anterior waves of expression, with each wave having a periodicity of the time needed to make one somite. The dynamic expression of *hairy1* is not dependent upon protein synthesis, suggesting that *hairy1* expression is an output of the clock rather than part of the clock itself (Palmeirim et al., 1997). Since then, several other genes have been shown to have a similar 'cycling' expression pattern, including *hes*, *her* and *hey* family members in zebrafish, chick and mouse (Holley et al., 2000; Jouve et al., 2000; Leimeister et al., 2000; Bessho et al., 2001a; Bessho et al., 2001b), *lunatic fringe* in chick and mouse (McGrew et al., 1998; Forsberg et al., 1998; Aulehla and Johnson, 1999), and *delta* homologs (*deltaC* and *deltaD*) in zebrafish (Jiang et al., 2000).

We have undertaken a genetic approach to understanding the role of *hairy/E(spl)*-related (*her*) genes during somitogenesis in zebrafish. We have isolated a deficiency, *b567*, that deletes both *her1* and *her7* genes. Like other Notch pathway mutants in mouse and zebrafish (Evrard et al., 1998; Kusumi et al., 1998; Zhang and Gridley, 1998; Durbin et al., 2000; Holley et al., 2000; Jiang et al., 2000) and the mouse *Hes7* knockout (Bessho et al., 2001b), *b567* mutant embryos show a disruption in somite anterior-posterior (AP) polarity. This disruption is phenocopied by injection of MOs (Nasevicius and Ekker, 2000) against *her1 + her7*. The abnormal expression of *deltaD* and *deltaC* in *her1+7* MO-injected embryos indicates that coordinated expression of *delta* cycling genes requires *her* genes. Thus, *her1* and *her7* may feed back into the clock as well as being a potential output of the clock. Injection of either *her1* or *her7* MOs indicates a partial functional redundancy for these genes. However, *her1* is necessary for the formation of the most anterior somite boundaries and *her7* is required for the normal formation of more posterior somite boundaries. In contrast to the fused somites-type mutants *bea*, *des* and *aei/deltaD*, where a number of anterior somites are spared, somitic defects in *b567* mutant and MO-injected embryos span the entire body axis. In both *b567* mutant embryos and *her1+7* MO-injected embryos, all somites are larger in the AP dimension than wild-type somites. These enlarged somites are delineated by stronger boundaries with at least one weak boundary attempt within the large somite. Thus, *her1+7*-deficient embryos have an 'alternating boundary' phenotype of strong boundary/weak boundary/strong boundary, demonstrating that *her1* and *her7* are essential for normal segmentation in zebrafish.

MATERIALS AND METHODS

Zebrafish mutant alleles, stocks and husbandry

Zebrafish embryos were obtained from natural spawnings of adult fish kept at 28.5°C on a 14 hour light/10 hour dark cycle and were staged according to Kimmel et al. (Kimmel et al., 1995). The homozygous *b567* mutation was isolated during a large scale mutagenesis screen of haploid progeny of F_1 females derived from γ-ray mutagenized males (see Walker, 1999). At approximately 10-11 hours post-fertilization (hpf), 20 haploid embryos from each clutch were fixed overnight in 4% paraformaldehyde (PFA) in phosphate-buffered saline (PBS) and dechorionated. Embryos were processed by in situ hybridization to detect transcripts of six genes: *hatching gland 1* (*hgg1*) (Thisse et al., 1994), *floating head* (*flh*) (Talbot et al., 1995), *pax2.1* (Krauss et al., 1991), *valentino* (*val*) (Moens et al., 1998), *fkh6* (Odenthal and Nüsslein-Volhard, 1998), and *her1* (Müller et al., 1996). In situ hybridization was performed as described below, either in Eppendorf tubes or in BEEM capsule baskets (see Moens et al., 1996). We focused on mutations that specifically disrupted *her1* gene expression and describe one mutation, *b567*.

Mapping the *b567* deficiency

DNA samples were prepared from *b567*$^+$ and *b567*$^-$ diploid and haploid embryos (Postlethwait et al., 1994). PCR using *her1* mapping primers (forward 5′-CAATCCTCTCAACCACGGAC-3′ and reverse 5′-ACAGCAAAGACCCCAGAACA-3′) amplified the expected 638 bp product from 28 *b567*$^+$ embryos and failed to amplify a product from 18 *b567*$^-$ embryos. Other Linkage Group 5 (LG5) markers were similarly tested to estimate the size of the deficiency. Primer sequences used for mapping (Fig. 1) can be retrieved from the Zebrafish Information Network (ZFIN), the Zebrafish International Resource Center, University of Oregon, Eugene, OR 97403-5274; World Wide Web URL: http://zfin.org/ (see Sprague et al., 2001) or from the authors.

Morpholino injections

Morpholino-modified antisense oligonucleotides (MOs) were designed and synthesized by Gene-Tools, LCC. Antisense sequences and locations relative to the start site are:

her1a MO, 5′-GACTTGCCATTTTTGGAGTAACCAT-3′ location: +1 to +25;

her1b MO, 5′-ACACCTTCAGTATTGTATTCCCGCT-3′ location: –49 to –24;

her7a MO, 5′-TCAATGAGGATATGATTCCAGAAAA-3′ location: –50 to –25;

her7b MO 5′-TTTCAGTCTGTGCCAGGATTTTCAT-3′ location: +1 to +25;

her4 MO 5′-AGGAGTCATTGCTGTGTGTCTTGTG-3′ location –16 to +9.

MOs were solubilized in water to a stock concentration of 50 mg/ml. The stock solution was diluted to a working concentration of 0.5-5 mg/ml in 1× Danieau solution as described (Nasevicius and Ekker, 2000) and supplemented with 0.1% Phenol Red (Sigma). In experiments where several MOs were injected together, the diluted single Danieau MO solutions were mixed in equimolar concentrations prior to microinjection. Zebrafish embryos were injected with 2-3 nl of the Danieau MO solution or Danieau control (no morpholino) at the 1-4 cell stages. Note that *her1* MO-injected embryos refers to embryos injected with *her1a* and *her1b* MOs and *her7* MO-injected embryos refers to embryos injected with *her7a* and *her7b* MOs.

In situ hybridization and immunocytochemistry

Whole-mount in situ hybridization was performed as previously

described (Jowett, 1999). F59 was used to visualize myosin fibers as previously described (Crow and Stockdale, 1986; Devoto et al., 1996). β-catenin antibody staining was performed as described (Topczewska et al., 2001). The original micrographs of β-catenin staining were inverted in Adobe Photoshop to facilitate visualization of the pseudocoloring (also performed in Adobe Photoshop).

Analysis of somite development

Live 14- to 18-somite embryos were mounted on a double-bridged slide (a coverslip with 2 adhered 1 μm coverslips) in 0.004% Tricaine in embryo medium (Westerfield, 1995). The embryos were then viewed in succession under the microscope. An acetate sheet was taped to the monitor and the somites traced. Somite boundary formation was judged by focusing medially and laterally to gain a three dimensional view of boundary formation. Strong boundaries were denoted with solid lines and weak boundaries were denoted with dashed lines. New acetate sheets were used for additional time points. At the conclusion of the time lapse, these sheets were aligned with each other (the yolk plug and tail were also traced to facilitate alignment), taped on a computer monitor, and traced using Adobe Photoshop.

RESULTS

Somite formation is disrupted in a zebrafish deficiency mutant that deletes two *her* genes, *her1* and *her7*

In a haploid-based screen designed to identify mutations affecting early embryonic gene expression (see Materials and Methods), we recovered a γ-ray-induced deficiency, *b567*, that specifically abolishes expression of a *hairy-related* gene, *her1* (Fig. 1). The *her1* gene is normally expressed in two or three stripes in the PSM of wild-type embryos (Muller et al., 1996), but *hairy/E(spl)*-related expression is not detected in *b567* mutant embryos (Fig. 1A,B). Several other genes were included in our in situ hybridization cocktail (see Fig. 1 legend); these genes are expressed normally in *b567* mutant embryos (Fig. 1A,B). Somite boundary defects are observed in *b567* mutant embryos at all stages of somitogenesis (Fig. 1C,D). Overall morphology in *b567* mutant embryos, however, is relatively normal during the first day of development, suggesting that the effect on somitic gene expression and somitogenesis is specific. *b567* mutant embryos do twitch. Generalized neural degeneration begins after the first day of development in *b567* mutant embryos, and mutant embryos die between 80-120 hours post-fertilization (data not shown). Later phenotypes have not yet been examined in detail.

Because *her1* is not expressed in *b567* mutant embryos, we suspected that the *b567* deficiency might delete the *her1* gene. Using a PCR strategy (see Materials and Methods), we confirmed that *her1*, and other closely linked markers on Linkage Group 5, were missing on the *b567* deficiency chromosome (Fig. 1E). One of the additional deleted genes is *her7*, another *hairy/E(spl)*-related gene that is expressed in a highly overlapping pattern with *her1* (M. U., unpublished; M. Gajewski, D. Sieger, B. Alt, C. Leve, S. Hans, C. Wolff, K. Rohr and D. Tautz, personal communication). The *b567* deficiency also deletes the *ndr3* gene and a number of ESTs for which gene expression data is not available (Fig. 1E). The resolution of the genetic map in the region is somewhat uncertain, but we have localized the proximal breakpoint of the deficiency to a 0.1-3.9 cM interval near *her1* and *her7*. The

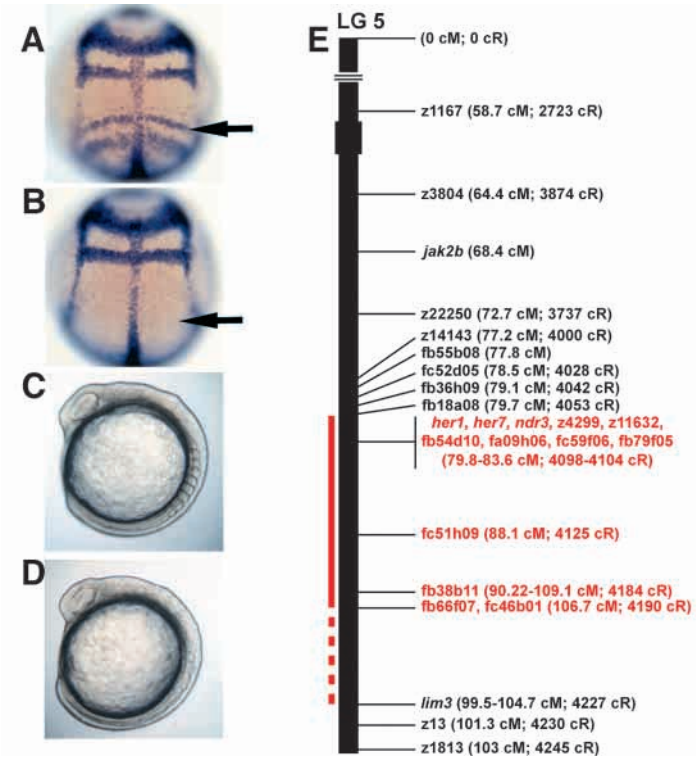

Fig. 1. *her1* and *her7* are included in the *b567* deficiency and *b567* mutant embryos have somitic defects. (A,B) Dorsal view of embryos hybridized with an in situ hybridization screen cocktail including *pax2*, *forkhead6*, *floating head*, *valentino* and *her1*. (A) Wild-type embryo; (B) *b567* mutant embryo lacking *her1* expression (arrows). (C,D) Although somite formation is disrupted in *b567* mutant embryos (D) as compared to wild-type embryos (C), overall embryo morphology is normal at this stage. (E) Map of the *b567* deficiency. A total of 25 markers, including SSLPs (z-markers), ESTs (prefixed by fa, fb and fc), and cloned genes (italicized), were PCR-amplified from DNA prepared from $b567^{+}$ and $b567^{-}$ embryos. Markers that failed to amplify from $b567^{-}$ DNA samples are indicated in red. Map positions are indicated in cM (indicating relative position on the integrated map [ZMAP] that includes all 6 independent mapping panels) and in cR (indicating position on the T51 mapping panel, on which 18 of the tested 25 markers have been mapped). Approximate centromere position is indicated by a thick black box. The solid red line indicates the extent of the deficiency and the dashed red line indicates the possible location of the telomeric breakpoint. The *b567* deficiency deletes approximately 92-174 cR (~15-22 cM) of LG 5.

distal breakpoint is located within a larger interval, but the mapping data together allows us to estimate that the deletion is not any larger than ~22 cM. Because a large number of genes could be absent in a 22 cM interval, we next used an antisense morpholino approach to identify which genes were likely responsible for the mutant somitic phenotype.

The somitic phenotype of *b567* is due to the deletion of *her1* and *her7*

As shown in Fig. 1, *b567* is a deficiency that results in the deletion of a number of genes. Both *her1* and *her7* are transcribed in the PSM, suggesting that these genes may function in somitogenesis and their loss may be responsible for the segmentation defects in *b567* mutant embryos. To test this hypothesis, we inhibited *her1* and *her7* mRNA translation by

Table 1. *her1* and *her7* 'knockdown' mimics the b567 somite phenotype

Antisense morpholino (MO)*	Dose (ng)	Total no. of embryos	No. of experiments	Somite phenotype of embryos at ~18 hours†		
				Normal somite morphology (%)	Partial somite disruption (%)	'Full' somite disruption (%)
Control	0	692	26	99	1	0
her1‡	2	56	2	85	15	0
her1‡	4	17	1	59	41	0
her1‡,**	6	63	3	30	70	0
her1‡,**	10	35	3	0	100	0
her7§	2	33	2	48	52	0
her7§	4	24	1	58	42	0
her7§,††	6	48	3	15	85	0
her7§,††	10	30	3	0	100	0
her1‡+*her7*§	1+1	164	5	4	40	55
her1‡+*her7*§	2+2	41	4	2	10	88
her1‡+*her7*§	3+3	169	6	0	0	100
her1‡+*her7*§	5+5	74	4	0	3	97
her4¶	2	97	3	81	19	0

*Morpholinos were diluted in 1× Danieau solution containing 0.1% Phenol Red to a final concentration of 1-3 ng/nl and approximately 2 nl was injected into the yolk cell at the 1-2 cell stage (Nasevicius and Ekker, 2000). Controls were injected with 1× Danieau containing 0.1% Phenol Red.

†Embryos with normal overall morphology at ~18 hours were scored. Partial somite disruption indicates that somite boundary defects were observed, but not along the entire axis. 'Full' somite disruption is equivalent to the *b567* somitic phenotype.

‡Mixture of two antisense morpholinos (*her1a* and *her1b*) of equal concentration.

§Mixture of two antisense morpholinos (*her7a* and *her7b*) of equal concentration.

¶*her4*-MO-injected embryos often have multiple morphological defects; at a dose of 4 ng, all embryos die before somitogenesis. Most embryos scored do not display a normal overall morphology; thus, the abnormal somite phenotype in some embryos may reflect general patterning defects.

**The first 1-4 anterior somite boundaries in *her1*-MO injected embryos appear to be enlarged or disrupted.

††Somites in the posterior trunk and tail are enlarged in the AP dimension

injecting morpholino antisense oligonucleotides (MOs) into zebrafish embryos (Nasevicius and Ekker, 2000). Two non-overlapping MOs were designed for both *her1* (*her1a* MO and *her1b* MO) and *her7* (*her7a* MO and *her7b* MO). Injection of all four MOs (*her1+her7*) perturbed formation of all somites (Table 1) and mimicked the *b567* mutant somitic phenotype. Injection of equivalent or higher dose of a *her1* MO combination (*her1a* MO+*her1b* MO) or a *her7* MO combination (*her7a* MO and *her7b* MO) failed to phenocopy the *b567* mutant somitic phenotype (Table 1). Injection of *her1* MOs produced slight morphological defects in anterior somites (somites 1-3), whereas injection of *her7* MOs caused boundary defects in posterior somites caudal to somite 11. As a control, a morpholino targeted against *her4*, which is only weakly expressed in the PSM (Takke and Campos-Ortega, 1999), was also tested. Most embryos injected with *her4* MOs displayed normal somite morphology. *her4* MO-injected embryos that did show segmentation defects also had extensive generalized disruption suggestive of MO toxicity. These results indicate that the segmentation defects in *b567* mutants are likely caused by the specific lack of *her1* and *her7*. The observation that *her1* and *her7* MOs individually produce distinguishable somitic phenotypes, but together mimic the *b567* mutant phenotype at lower doses than the single injections (Table 1) suggests that *her1* and *her7* have partially, but not completely, redundant functions.

Segmental expression of paraxial mesoderm genes is disrupted in *b567* mutant and MO-injected embryos

Paraxial mesoderm specification in *her1+7* MO-injected embryos appears normal, as expression of *spt* and *tbx6* (Griffin et al., 1998; Hug et al., 1997) in *her1+7* MO-injected embryos is indistinguishable from control-injected embryos (data not shown). As somitogenesis is disrupted in *her1+7* deficient embryos, we next examined whether anterior-posterior (AP) somite polarity and expression of cycling genes was normal in *her1+7*-deficient embryos (Fig. 2). *myoD* and *paraxial protocadherin* (*papc/pcdh8*) are markers of posterior and anterior somite polarity, respectively (Weinberg et al., 1996; Yamamoto et al., 1998). Segmental *myoD* expression in the posterior half of formed somites is disrupted in both *b567* mutant and *her1+7* MO-injected embryos. In these embryos, *myoD* expression is not restricted to the posterior half of formed somites and is instead expressed in all paraxial cells (Fig. 2A-D). In wild-type embryos, *papc* is segmentally expressed in the presumptive anterior half of the next two somites that will form (Fig. 2E,G). In both *her1+7* MO-injected and *b567* mutant embryos, *papc* is expressed broadly throughout the anterior PSM (Fig. 2F,H). In wild-type embryos, ephrin receptor *ephA4* and ligand *ephrin B2* expression is refined to stripes denoting the anterior and posterior aspects, respectively, of mature somites and the next presumptive somite (Durbin et al., 1998). In contrast, both *ephA4* (data not shown) and *ephrin B2* (Fig. 2Q,R) are expressed throughout the paraxial mesoderm of *her1+7* MO-injected embryos. Thus, the AP polarity of somites is disrupted in *her1+7*-deficient embryos.

Previous analysis of Notch signaling pathway mutants demonstrated that disruption of one component can affect the expression of other Notch pathway genes (Zhang and Gridley, 1998; Hrabe De Angelis et al., 1997; Holley et al., 2000). For example, Delta signaling is required for the dynamic expression of *hairy/E(spl)*-related genes in both mouse and zebrafish (Jouve et al., 2000; Holley et al., 2000). Interestingly, *Hes7*, but not *Hes1*, is required for dynamic expression of

lunatic fringe (Bessho et al., 2001; Jouve et al., 2000). We examined whether expression of Notch pathway components was affected in *b567* mutant and *her1+7* MO-injected embryos. The expression of *notch5*, normally a posterior somite polarity marker in wild-type embryos, is much more uniformly expressed in *her1+7* MO-injected embryos (Fig. 2M,N). In wild-type embryos, both *deltaC* and *deltaD* are dynamically expressed in the posterior PSM but the expression of these genes becomes fixed in the anterior PSM in the posterior or anterior half of the next presumptive somite, respectively (Jiang et al., 2000). In *b567* mutant and *her1+7* MO-injected embryos, *deltaD* is expressed in a broad band in the anterior PSM rather than in discrete stripes as in wild-type embryos (Fig. 2I,J, and data not shown). The expression of *deltaC* in the anterior PSM is also seen in a large band in *her1+7* MO-injected embryos (Fig. 2K,L). The pattern of expression does not vary among *her1+7*-deficient embryos, suggesting that there is no coordinated dynamic expression of *deltaC* or *deltaD*. In mouse, *Mesp2*, a gene encoding a basic helix-loop-helix protein, is expressed in the presumptive rostral region of somite minus 1 (the somite that will form next) and has been shown to interact genetically with the Notch pathway (Takahashi et al., 2000). The expression of *mespA* in *b567* mutant embryos resembles the *mespA* expression in both *bea* and *mib* mutant embryos: there is one broad domain of reduced expression rather than in 2 sharp bands as in wild-type embryos (Fig. 2O,P) (Sawada et al., 2000). Thus, *her1* and *her7* are required for segmental expression of both Notch pathway genes and the specification of AP polarity.

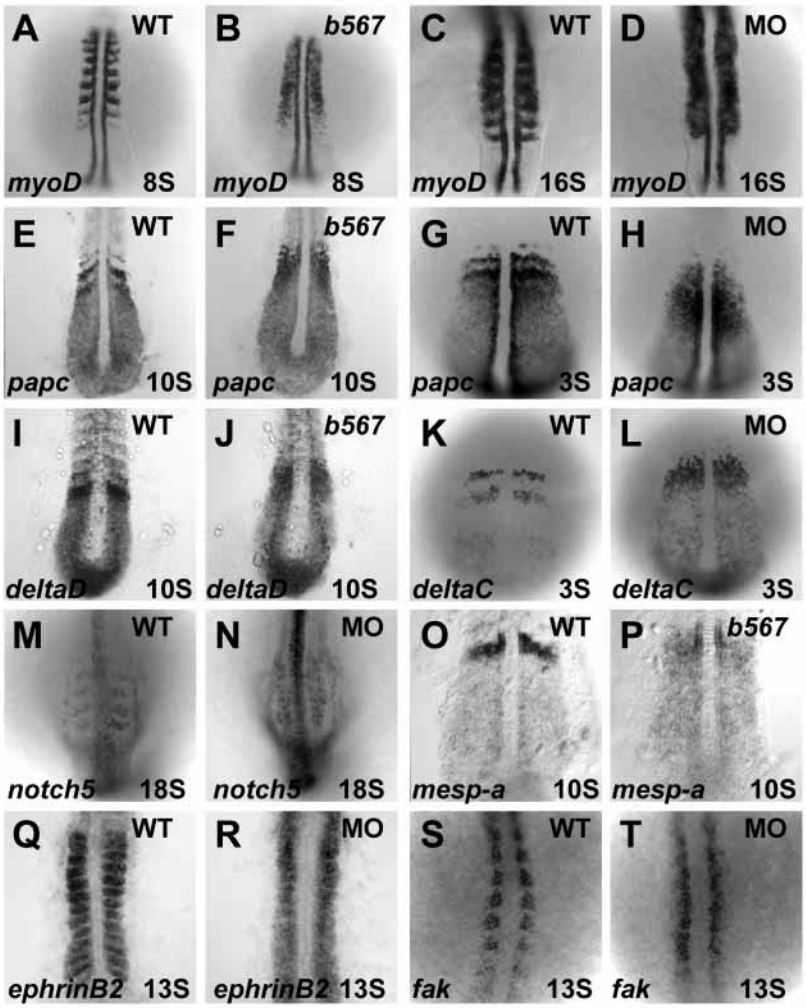

Fig. 2. AP patterning of somites is disrupted in *her1+7* MO-injected and *b567* mutant embryos. WT denotes wild-type embryos, and MO denotes *her1+7* MO-injected embryos. All panels are dorsal views with anterior towards the top. Developmental stages are indicated at the bottom right. The segmental expression of *papc* and *myoD* is disrupted throughout somitogenesis in MO-injected and *b567* mutant embryos (A-H). The Notch ligands *deltaD* and *deltaC* are expressed throughout the presumptive somite rather than being restricted to the anterior or posterior half, respectively (I-L). Expression of a Notch receptor, *notch5*, is also disrupted (M,N). In addition, the expression of *mespA* is downregulated and not segmental in *b567* mutant embryos (O,P). Both *ephrin B2* (Q,R) and *fak* (S,T) are expressed throughout the paraxial mesoderm instead of in posterior half-somites.

As *hairy/E(spl)*-related genes are transcriptional repressors that feedback on Notch signaling (reviewed by Davis and Turner, 2001), one prediction would be that outputs of Notch signaling other than *her1* and *her7* should be activated in *her1+7* MO-injected embryos. Zebrafish *focal adhesion kinase* (*fak*), shows a specific response to activation of the Notch pathway via activated *Suppressor of Hairless* (*X-Su(H)1/Ank*) and not to inhibition of the Notch pathway via a dominant negative *Suppressor of Hairless* (*X-Su(H1)*^{DBM}) (Henry et al., 2001; Wettstein et al., 1997). The expression of *fak* in *her1+7* MO-injected embryos resembles that of embryos injected with activated *Supressor of Hairless*, suggesting that the Notch pathway may be activated in *her1+7* MO-injected embryos (Fig. 2S,T).

Somites in *her1+7* MO-injected and *b567* mutant embryos are enlarged in the AP dimension

In wild-type embryos, somites form with a regular temporal and spatial periodicity (Fig. 3A). In *b567* mutant embryos, somites are enlarged in the AP dimension (Fig. 3B). There appear to be weak (incomplete) boundaries within the stronger (though imperfect) boundaries that delineate the large somites (Fig. 3B, arrowheads). Immunohistochemistry using F59 to stain myosin fibers (Crow et al., 1986; Devoto et al., 1996) affirms that somites in *b567* mutant embryos are enlarged in the AP dimension compared to wild-type embryos (Fig. 3C,D). In wild-type embryos, muscle fibers span the length of one somite and terminate at the boundary of adjacent somites. In *b567* mutant and *her1+7* MO-injected embryos, muscle fibers cross boundaries and terminate within the myotome (Fig. 3C-E). Expression of a *titin* homolog that labels mature somite boundaries also reveals that somite periodicity is altered in *b567* mutant embryos. In wild-type embryos, chevron-shaped *titin* expression is regularly spaced along the AP axis (Yan et al., 2002). In *b567* mutant embryos, *titin* staining delineates somites that are poorly formed and enlarged in the AP dimension (Fig. 3F,G).

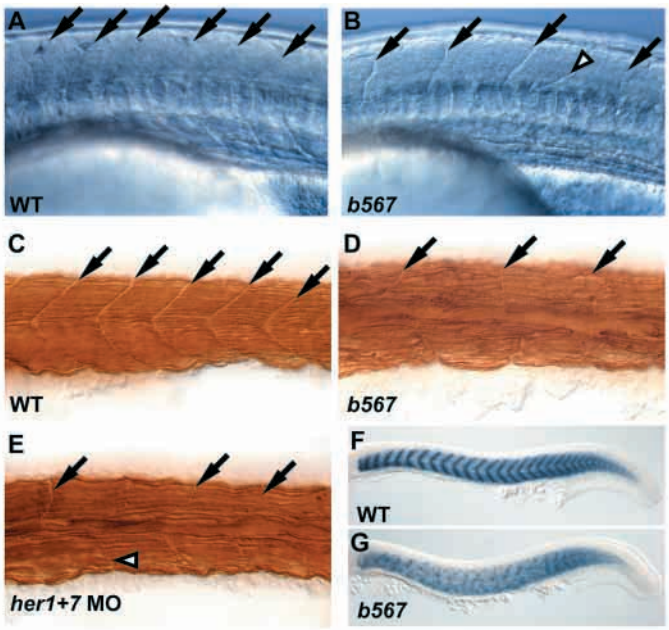

Fig. 3. Somites in *b567* mutant embryos are enlarged in the AP dimension. Whereas live 24 hpf wild-type embryos have reiterated somites over regular intervals (A, arrows), *b567* mutant embryos (B) have enlarged somites (arrows) with weak boundaries in between (arrowhead). (C-E) F59 staining highlights the large, irregular boundaries in both *b567* mutant and *her1+7* MO-injected embryos. Again, arrows denote strong boundaries and arrowheads denote weak boundaries. Molecular evidence of large somites is seen by expression of a *titin* homolog (F,G).

We have observed that *b567* mutant embryos have imperfect somites that are enlarged in the AP dimension. In addition, weak boundaries appear to form within the enlarged somites. In order to more carefully assess the function of *her* genes in somite morphogenesis, we analyzed somite morphology at the cellular level in *her1+7* MO-injected embryos by using an antibody against β-catenin (Topczewska et al., 2001). We asked two questions: where are boundaries forming in these embryos, and what is the morphology of the boundaries that do form? Unlike wild-type boundaries, the boundaries that form in *b567* mutant or *her1+7* MO-injected embryos are not fully extended in either the dorsal-ventral or medial-lateral dimensions. We therefore defined a strong somite boundary in *her*-deficient embryos as one that extends at least 90% of the dorsal-ventral dimension and occupies one third of the mediolateral dimension. Somites in *her1+7* MO-injected embryos are consistently larger in the AP dimension compared to wild-type embryos (Fig. 4). While it is sometimes observed that a somite of wild-type size does form in between large somites (data not shown), the average spatial periodicity of somites in *her1+7* MO-injected embryos is approximately one and a half to two somite equivalents (Fig. 4). Weak boundaries in the middle of the large somites were observed in *her1+7* MO-injected embryos (arrowheads, Fig. 4D,F). These weak boundaries are defined as such because they appear to be formed from a few cells lining up but do not extend in the dorsal-ventral or mediolateral dimension. The observation of weak boundaries within the large somites suggests a strong boundary/weak boundary/strong boundary segmentation pattern in these embryos. Thus, analyzing somite formation in *her*-deficient embryos at high resolution has revealed a consistent pattern in what might otherwise be characterized as merely disrupted somites. In wild-type embryos, somitic boundaries are formed via the alignment and epithelialization of presumptive border cells (Henry et al., 2000). A boundary is thus flanked by a neat row of rectangularly shaped border cells (Fig. 4B). Boundaries in *her1+7* MO-injected embryos are also flanked by rectangular, aligned border cells (Fig. 4D,F). Although the border cells in *b567* mutant embryos are slightly more disorganized, aligned rectangular cells do flank the strong boundaries. This indicates that *her1* and *her7* are not necessary for border cell morphogenesis. However, *her1* and *her7* may be necessary for the refinement and strengthening of alternate somite boundaries.

The stronger boundaries observed in *her1+7* MO-injected embryos extend further in the dorsal-ventral dimension than those of *b567* embryos. The difference could be explained by (1) incomplete inhibition of *her* mRNA translation in MO experiments or (2) the deletion of another gene in the *b567* deficiency. If the first scenario accounts for the differences observed, we would postulate that alternate somite boundaries are more sensitive to a decrease in *her1+7* activity. In the second scenario, we would postulate that an additional gene that is deleted in the *b567* deficiency is required to facilitate alignment of border cells in the dorsal-ventral dimension.

her1 functions in anterior somite formation, while *her7* functions in posterior somite formation

The observation that somites in *her1+7* MO-injected and *b567* mutant embryos are enlarged in the AP dimension led us to analyze the specific defects in embryos injected with either *her1* or *her7* MOs. Most somites in *her1* MO-injected embryos are well formed with normal periodicity (Fig. 5A), however, the anterior-most somites are defective. There is a range of defects observed, from fusion of either somites 1 and 2 or somites 2 and 3, to disrupted boundary formation among these somites. This relatively subtle but consistent effect of *her1* MOs strongly suggests there is an early role for *her1* for which *her7* cannot compensate. In *her7* MO-injected embryos, the two most recently formed somites are clearly enlarged (Fig. 5B). Analysis of somite formation in *her7* MO-injected embryos at later stages (18-24 somites) also indicated a clear trend of 'strong boundary/weak boundary/strong boundary/weak boundary' (blue and red boundaries in Fig. 5C, respectively). Somites anterior to somite 11 were normally formed. This indicates that *her1* cannot compensate for *her7* in the posterior trunk and tail.

In *her1*+7 MO-injected embryos, somites along the entire AP axis are enlarged (Fig. 4C,E) and *deltaD* expression is disrupted in early and late somitogenesis (Fig. 5G, and data not shown). Embryos injected with *her7* MOs, however, only display morphological segmentation defects late in segmentation (Fig. 5B,C). We therefore tested the hypothesis that *deltaD* expression would be normal early in somitogenesis but disrupted later. Indeed, this was the case. At the 2-somite stage, two *deltaD* stripes (similar to those in wild-type embryos) were observed in the anterior PSM in *her7* MO-injected embryos (Fig. 5D,E); whereas, at the 10-somite stage, one large *deltaD* band, instead of two smaller bands, is observed (Fig. 5I). Thus, inappropriate *deltaD* expression

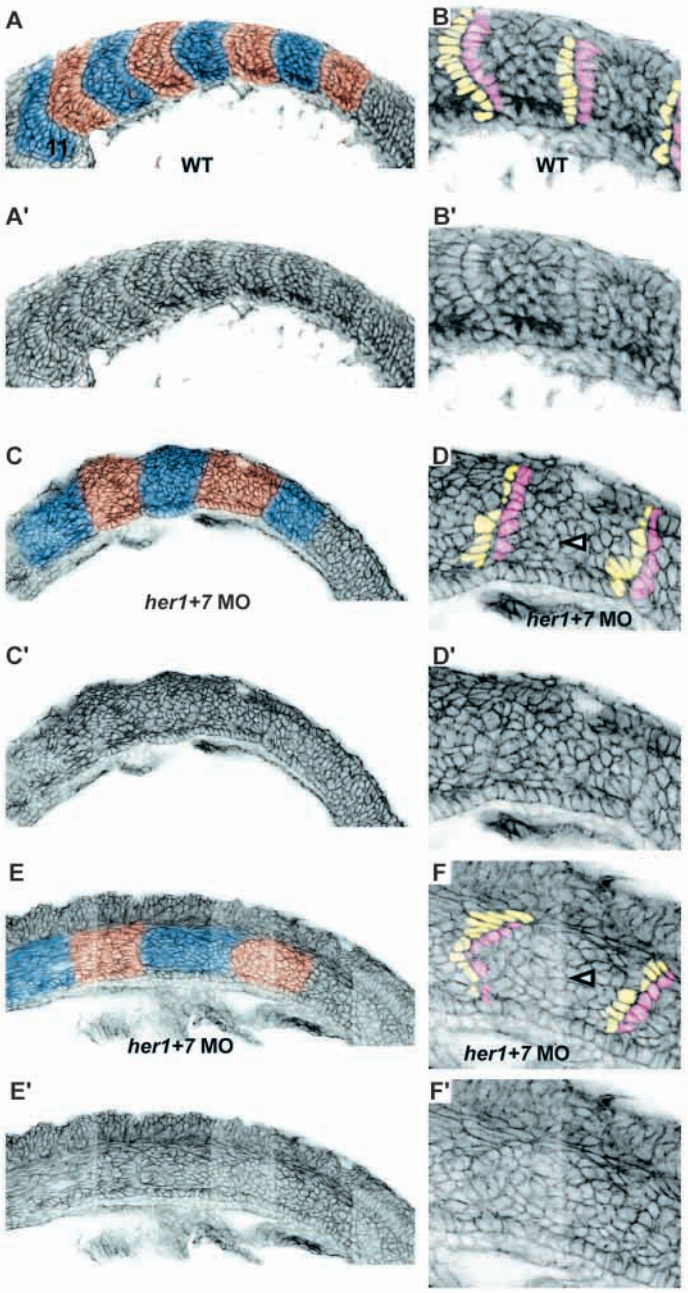

Fig. 4. Somites in *her1+7* MO-injected embryos are enlarged in the AP dimension. All panels are confocal micrographs with black and white inversed, side views of β-catenin staining in 17- to 18-somite embryos. A′-F′, are the same confocal micrographs as A-F, without any pseudocoloring. (A,B) Wild-type embryo. (A) Anterior somites are chevron-shaped and posterior somites are more block shaped. Red-brown and blue colors denote alternating somites. The anteriormost somite shown in (A) is somite 11, panels C and E are at approximately the same AP position. (B) A higher magnification view of A showing the epithelial, cuboidal border cells (yellow and pink) that flank the intersomitic boundary. (C-F) *her1+7* MO-injected embryos. Somites in these embryos are larger in the AP dimension. It is important to note that the stronger somite boundaries that are denoted by pseudocoloring are defined as such by their 3-dimensional structure: these boundaries occupy at least 90% of the dorsal-ventral dimension and 30% of the mediolateral dimension (as determined by viewing all of the focal planes, not just the one shown). (D,F) Some weak attempts at boundary formation in between stronger boundaries (arrowheads) are seen in these confocal sections. The weak boundaries do not meet our stronger boundary criteria.

correlates well with the commencement of somite boundary defects in *her7* MO-injected embryos. Interestingly, we also observed milder disruption of presomitic *deltaD* expression at the 10-somite stage in *her1* MO-injected embryos (Fig. 5H). However, the somitic expression of *deltaD* in *her1* MO-injected embryos is segmental.

Selective strengthening of boundaries underlies the large somites in *her7* MO-injected embryos

The phenotype of *her1+7* MO-injected embryos, alternating strong and weak boundaries, is quite intriguing. There are at least 2 possibilities to explain this observation. First, the strong boundaries could delineate large somites and then the weak boundaries could subdivide the large somites. Alternatively, weak boundaries could form and a subset of these boundaries could be strengthened. We analyzed somite formation over time and determined that the latter explanation is most likely. It has previously been shown that somite boundary formation proceeds via the alignment of clefts (Wood and Thorogood, 1994). The clefting of strong boundaries in *b567* mutant and *her1+7* MO-injected embryos, although much more evident than clefting of weak boundaries, does not occupy the entire mediolateral extent of somites and is best visualized in three dimensions by focusing through the entire mediolateral extent of the somite. We followed somite development by tracing the boundaries of live embryos approximately every 30-40 minutes (see Materials and Methods). We followed somite development in *her7* MO-injected embryos because the posterior somites in these embryos resemble those in *her1+7* MO-injected embryos but somite boundaries are easier to visualize.

In wild-type embryos, a new strong somite boundary was seen approximately every half hour (n=7 boundaries in 2 embryos) (Fig. 6A,D). Because tracings were made every 30-40 minutes, a new strong boundary that occupies the entire dorsal-ventral and mediolateral extents of the PSM had usually formed in wild-type embryos (Fig. 6A,D). We also sometimes observed weak clefting as a wild-type boundary was forming (data not shown). Strong boundary formation was observed in *her7* MO-injected embryos (n=18 strong somite boundaries formed in 5 embryos), however, there was more variability in timing of boundary formation than in wild-type embryos as shown in Fig. 6B and C. Furthermore, somite boundary formation in these embryos was delayed relative to wild-type embryos (data not shown).

Somites in *her7* MO-injected embryos are enlarged in the AP dimension, yet weak boundaries are observed within these large somites (Fig. 5). In order to understand the role of *her* genes in somite formation it is necessary to analyze when these weak boundaries are forming relative to the strong boundaries. As outlined above, one possibility is that after a large somite forms in *her7* MO-injected embryos, it subsequently becomes subdivided. If this were true, we would visualize strong boundary formation (delineating a large somite) prior to weak boundary formation within the large somites. This was not observed in *her7* MO-injected embryos. Instead, weak

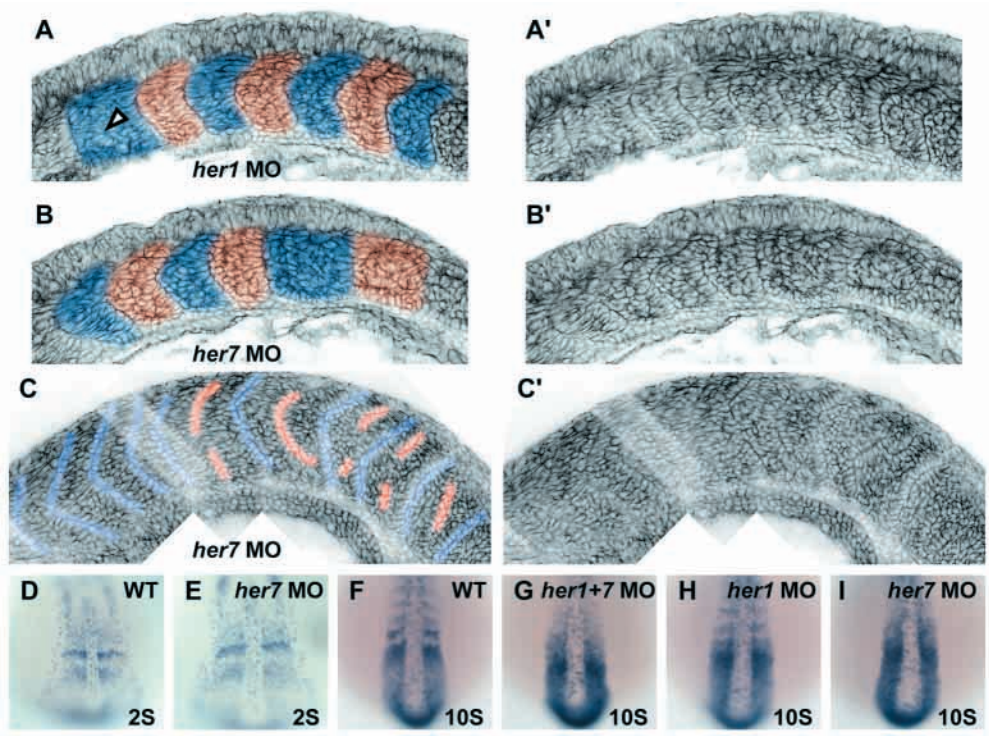

Fig. 5. *her1* and *her7* are partially redundant. (A-C) Confocal micrographs, side views of embryos stained for β-catenin to outline cell boundaries. A′, B′ and C′ are non-colorized versions of the confocal micrographs. (A) The first 2-3 somites in *her1* MO-injected embryos (15 somite stage) are disrupted. The arrowhead denotes an attempt at a somite boundary that does not extend fully in either the mediolateral or dorsoventral dimensions. All other boundaries appear normal. (B) While anterior somites are normal in *her7* MO-injected embryos (15 somite stage), posterior somites are enlarged. The first somite shown is somite 9. (C) Interior boundaries partially recover over time in *her7* MO-injected embryos (22 somite stage). Strong boundaries are highlighted in blue. Weak boundaries are shown in red. (D-I) *deltaD* expression correlates with abnormal somite morphology in *her7* MO-injected embryos. Early *deltaD* expression (2 somite stage) is unaffected in *her7* MO-injected embryos compared to control embryos (D,E), but later (10 somite stage), *deltaD* expression is disrupted (F,I) similar to *her1+7* MO-injected embryos (G). Interestingly, presomitic mesoderm expression of *deltaD* is partially disrupted in *her1* MO-injected embryos (H), but somite morphology is normal posterior to somite 3 (A).

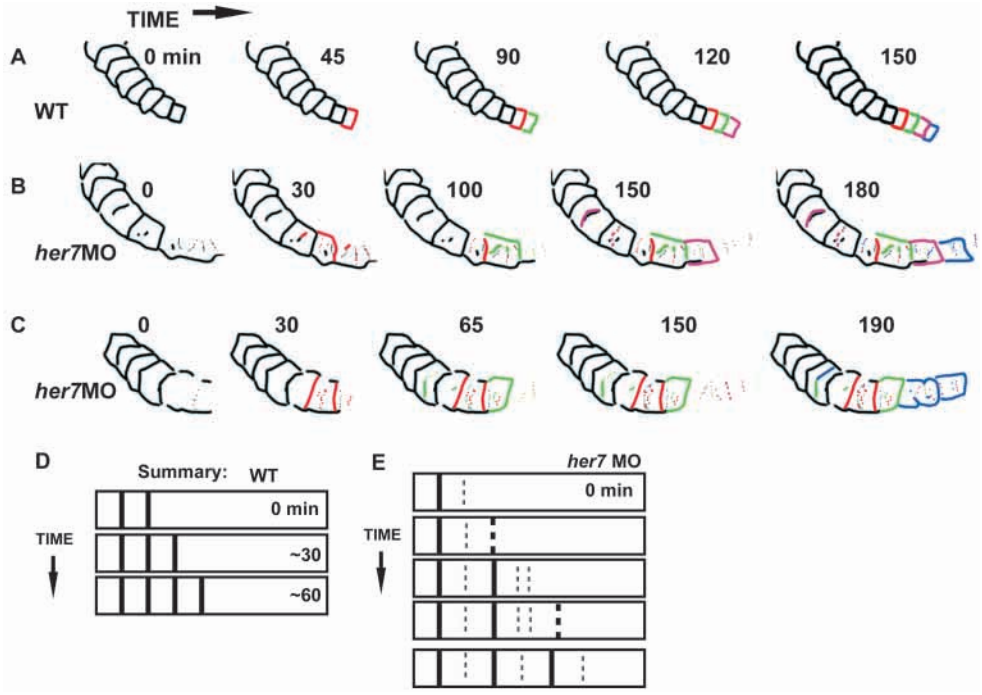

Fig. 6. Alternate somite boundaries are strengthened in *her7* MO-injected embryos. Embryos were examined approximately every 30-40 minutes. The somites that had formed at the beginning of the experiment (A,B,C) are shown in black. Anterior is towards the top and left in A-C, and at the left in D,E. Development at the first time point is shown in red, the second in green, the third in pink, and the fourth in purple. In wild-type embryos (A), a strong somite boundary forms at every time point. Weak boundaries are sometimes seen as somites are forming, but were not observed in this particular embryo. In *her7* MO-injected embryos (B,C), somite boundary formation is altered in 3 ways. First, weak boundaries persist much longer than in wild-type embryos and are therefore more frequently observed (dashed lines). Secondly, weak and disorganized attempts form in a segmental fashion but only alternate boundaries are strengthened (solid lines). Finally, large somites sometimes subdivide into 2 normal somites after the formation of many more posterior somites. (D,E) A cartoon summary of somite formation in wild-type (D) and *her7* MO-injected embryos (E). In wild-type embryos, somites form in an anterior- to-posterior fashion approximately every 30 minutes. In *her7* MO-injected embryos, weak boundaries (dashed lines) form in a segmental fashion. However, only some weak boundaries are strengthened (solid lines).

boundaries were visualized before strong boundaries formed. Furthermore, most strong boundaries (82%) were preceded by weak boundaries at the same or similar location. Thus, in *her7* MO-injected embryos there are weak attempts at boundary formation that proceed in an AP progression, but only a subset of these attempts (approximately every other boundary) becomes strengthened.

DISCUSSION

We have isolated a deficiency that deletes the *hairy/E(spl)*-related genes *her1* and *her7*. Injection of antisense morpholino oligonucleotides demonstrates that the somitic phenotype of *b567* mutants is largely due to the deletion of *her1* and *her7*. Both *her1+7* MO-injected and *b567* mutant embryos display disrupted gene expression in the paraxial mesoderm and imperfect somites display a one and a half to two segment periodicity relative to wild-type embryos. Thus, *her1* and *her7* are required for normal somite formation.

A delineation of anterior and posterior half-segments may not be necessary for boundary formation

It has been proposed that the juxtaposition of anterior and posterior half-segments may determine where a somite boundary forms (Meinhardt, 1986; Durbin et al., 1998; Durbin et al., 2000; Jen et al., 1999). In support of this hypothesis, it has been shown that transplantation of cells expressing *ephrin A4*, a marker of anterior somite polarity, can locally rescue boundary formation in *fss* mutant embryos. *fss* mutant embryos are unique among the known zebrafish segmentation mutants as they form no somitic boundaries (van Eeden et al., 1996). In addition, anterior somite polarity markers are not expressed in *fss* mutant embryos; instead, markers of posterior polarity are expressed throughout the paraxial mesoderm (Durbin et al., 2000). In other zebrafish mutants, such as *bea*, *des*, *mib* and *aei/deltaD*, cells expressing anterior and posterior markers are intermingled in the mutant paraxial mesoderm, and mutant embryos fail to form somites in the posterior trunk and tail (van Eeden et al., 1996; van Eeden et al., 1998; Durbin et al., 2000; Holley et al., 2000). As in this latter class of mutants, markers of AP somite polarity are also misexpressed in *b567* mutant and *her1+7* MO-injected embryos. We have tested four anterior markers (*papc/pcdh8, deltaD, mespA, EphA4*) and five posterior markers (*myoD, deltaC, notch5, fak/ptk2, ephrin B2*) and the expression of all of these genes is continuous within the PSM and somitic mesoderm (Fig. 3). However, boundaries do form in *her1+7* MO-injected embryos (again, stronger boundaries extend at least 90% of the dorsal-ventral dimension and one third of the medial-lateral dimension). In *her1* MO-injected embryos, *deltaD* is correctly expressed in the mature somitic mesdoerm, but is not expressed in a tight band in the anterior half of the PSM. Despite this disruption in AP polarity of the PSM, somites in these embryos (except for the most anterior somites) form just as in wild-type embryos (Fig. 5). These data suggest that the somite that is about to form does not have to be subdivided into prospective anterior and posterior halves at the mRNA level in order for a boundary to form. However, we have not tested all markers of AP polarity. In addition, we currently lack the tools to determine if post-transcriptional mechanisms allow the expression of these proteins in the A or P half of the somite. Alternatively, there may be genes that have not yet been isolated that are expressed normally in the anterior and posterior halves of presumptive somites in *her1+7* MO-injected embryos.

The expression of *papc* and *deltaD* in wild-type embryos delineates the anterior half of a prospective somite (Holley et al., 2000; Yamamoto et al., 1998). A wide band of strong expression of both *deltaD* and *papc* is seen in *b567* mutant and MO-injected embryos. It is possible that this entire band of *deltaD* and *papc* expression is perceived in the presomitic mesdoerm as anterior identity and somite borders thus form at the juxtaposition of *papc/deltaD*-expressing cells with cells that do not strongly express *papc/deltaD*. Therefore, although intrasegmental polarity may not be necessary for segment formation, it is possible that the driving force behind the formation of enlarged somites is the formation of a boundary between a large group of cells expressing *papc* and those that are not (Kim et al., 1998). The formation of a weak boundary in between the strong boundaries could be due to the normal expression of genes involved in AP differentiation that are not yet identified or were not surveyed in this study.

her1 and *her7* function partially redundantly

The somitic phenotype of *b567* mutants is phenocopied via injection of MOs against *her1+her7*. Single injection of either *her1* MOs or *her7* MOs does not phenocopy the somitic defects seen in *b567* mutant embryos. The dose required to phenocopy the somitic defects of *b567* mutant embryos throughout the embryonic axis in *her1+7* MO-injected embryos is much less (3 fold) than the doses required to partially disrupt segmentation in embryos injected with either *her1* or *her7* MOs (Table 1). Thus, *her1* and *her7* appear to function redundantly. However, some defects in somitogenesis are observed in embryos singly injected with either *her1* MOs or *her7* MOs. In *her1* MO-injected embryos, the anteriormost somites are frequently fused suggesting that *her1* has an early function for which *her7* cannot compensate (Fig. 5). In *her7* MO-injected embryos, somites posterior to approximately somite 10-13 are enlarged in the AP dimension much as somites in *b567* mutant and *her1+7* MO-injected embryos are (Fig. 5). Thus, *her7* appears to have a late function for which *her1* cannot compensate. These data indicate that although *her1* and *her7* have partially redundant functions, they are both required for normal somitogenesis.

hairy/E(spl)-related genes encode transcriptional repressors that bind to DNA as either hetero- or homodimers (reviewed by Davis and Turner, 2001). The partial redundancy of *her1* and *her7* may be explained in light of the ability of these proteins to function as hetero- or homodimers. It is possible that either *her1* or *her7* homodimers may be sufficient for normal somite formation in much of the trunk but *her1* homodimers are not sufficient for normal somite formation in the tail. Alternatively, it is possible that other *her* genes such as *her4* or *her6* (Takke et al., 1999; Pasini et al., 2001) are upregulated and heterodimers including new combinations of Her proteins are sufficient for segmentation in the trunk.

The dynamic expression of *hairy1* in the PSM is not dependent upon protein synthesis (Palmeirim et al., 1997), suggesting that *hairy1* does not negatively regulate its own expression. However, it has been demonstrated that *Hes7*

promoter activity is increased in a *Hes7* knockout mouse and that *Hes7* can repress transcription in vitro (Bessho et al., 2001a; Bessho et al., 2001b). Furthermore, HES1 has been shown to negatively autoregulate its own transcription (Takebayashi et al., 1994). We have been unable to assess the effects of *her1* and *her7* on their own transcription because *b567* is a deficiency, and because our experiments suggest that *her1* and *her7* morpholinos stabilize the corresponding mRNA transcripts (data not shown). We have shown that *her4* MOs do not perturb segmentation (Table 1), but this does not preclude the possibility that upregulation of additional *her* genes (or other genes altogether) could account for the delayed formation of boundaries in *her1+7* MO-injected embryos.

Somites in MO-injected embryos form by selective strengthening of boundaries

We have shown that somite boundaries in *her1+7*-deficient embryos are enlarged in the AP dimension. The spatial periodicity of somite formation in these embryos is one and a half to two somites. By following somite development over time, we have observed that the stronger somite boundaries that do form in *her7* MO-injected embryos are formed via selective strengthening of weak boundaries (Fig. 6). We predict that the enlarged somites that form in *her*-deficient embryos also form by selective strengthening of weak boundaries. Combined, these data suggest that the *her1* and *her7* genes are necessary to form strong boundaries on schedule. Furthermore, *her1* and *her7* are necessary for the strengthening of alternate weak boundaries.

her genes and the segmentation clock

It was first demonstrated in chick that *hairy1* is expressed in repeating posterior to anterior progressing waves of expression (Palmeirim et al., 1997). Other Notch pathway genes are also expressed in waves, including *lunatic fringe* in the chick and mouse (Forsberg et al., 1998; McGrew et al., 1998; Aulehla and Johnson, 1999), *Hes1* and *Hes7* in the mouse (Jouve et al., 2000; Bessho et al., 2001a; Bessho et al., 2001b), *deltaD, deltaC* and *her1* in the zebrafish (Holley et al., 2000; Jiang et al., 2000; Sawada et al., 2000). The dynamic expression of *hairy1* and *hairy2* is not dependent upon protein synthesis (Palmeirim et al., 1997; Jouve et al., 2000). This observation has led to the suggestion that *hairy1* may not be a component of the clock but rather an output of the clock (Palmeirim et al., 1997; Jouve et al., 2000). *her1* expression does not oscillate in *aei/deltaD* embryos, indicating that *her1* may be downstream of Notch signaling (Holley et al., 2000). Thus, if *her1* is downstream of Notch signaling and an output of the clock, Notch signaling may be a component of the segmentation clock. We show that *deltaC* and *deltaD* do not cycle in *her1+7* deficient embryos. Thus, although *her1+7* may be direct outputs of the segmentation clock they also could feed back into the clock. Alternatively, Notch signaling, as well as *her1* expression, may also be an output of the segmentation clock. In this scenario, *her1+7* MOs may either feedback into the clock to eliminate *deltaC* and *deltaD* cycling, or these MOs may eliminate *deltaC* and *deltaD* cycling via constitutively activating Notch signaling.

Recently, it has been shown that FGF signaling encodes a 'determination front', the position of which affects the size of somites in both chick and zebrafish (Dubrulle et al., 2001; Sawada et al., 2001). FGF signaling in the posterior PSM keeps cells in an immature state. At a critical level of FGF signaling in the more anterior PSM, cells appear to become allocated to a particular somite. Thus, ectopic FGF in the PSM generates smaller somites, presumably by slowing down the reception of the 'wavefront' signal such that fewer cells are allocated into each somite. Conversely, inhibition of FGF signaling generates larger somites, and it was hypothesized that this affect was due to an increase in the number of cells that received the 'wavefront' signal. We have observed that *fgf8* expression in the tailbud of *her1+7* MO-injected embryos resembles that of wild-type embryos (data not shown). It thus seems to be unlikely that the enlarged somites in *b567* mutant and *her1+7* MO-injected embryos reflect changes in the 'determination front'. However, we have not investigated the expression of other *fgfs* or the activation of ERK in MO-injected embryos.

her genes and synchronization of the segmentation clock

It has been proposed that one role for Notch signaling in coordinating somite formation is to synchronize the oscillations between neighboring cells (Jiang et al., 2000). In *her1+7*-deficient embryos, a large band of upregulation of *deltaD* and *deltaC* is seen. This is presumably due to the lack of the transcriptional repressors encoded by *her1* and *her7*. If there were additional outputs of Notch signaling (such as *Enhancer of split-related* proteins [ESRs] as found in *Xenopus*) (Jen et al., 1999) then these outputs would be constitutively activated in the presence of the ligands *deltaC* and *deltaD*. The nonsegmental expression of *fak* in *her1+7* MO-injected embryos (Fig. 2) suggests that there are outputs of Notch signaling besides *her1* and *her7*. Thus, a larger group of cells may be synchronized and respond to the 'somite formation signal', or 'wavefront', by making a larger somite. The presence of a weak boundary forming in the middle of enlarged somites in *her1+7*-deficient embryos could reflect subtle differences in synchronization.

Similarities and differences in segmentation strategies

One outstanding question in the field of evolutionary developmental biology is how segmentation in different phyla has evolved. If a general consensus could be defined, it would probably be that somite formation is not analogous to segment formation in *Drosophila* (reviewed by Davis and Patel, 1999). The formation of enlarged somites with a one and a half to two segment periodicity in *her1+7* MO-injected embryos is thus a very interesting phenotype. It is unlikely that this phenotype reflects a strict pair rule function for *her1* and *her7* because it is sometimes observed that a normal segment is formed in between two large somites. Furthermore, not every large somite is the same size.

However, it is possible that *her* genes may play a role outside of Notch signaling in the formation of alternate boundaries during zebrafish segmentation. In *Tribolium castaneum*, a short germ band insect, mutants that display a pair rule phenotype have been isolated (Sulston and Anderson, 1996; Sulston and Anderson, 1998; Maderspacher et al., 1998). The *Tribolium itchy* mutant displays a clear strong boundary/weak boundary phenotype as assayed by *engrailed* expression and is missing odd thoracic

segments and a variable number of abdominal segments. The ability to identify the missing thoracic segments, combined with the reduced *engrailed* expression and missing abdominal segments allows classification of *itchy* as a pair rule gene. The first report of the expression of zebrafish *her1* showed that *her1* is expressed in a metameric pattern during somitogenesis. Furthermore, stripes of *her1* expression gave rise to alternating somitic primordia at the two stages examined (Müller et al., 1996), suggesting a potential role of *her1* as a pair rule-type gene. This suggests that one alternative possibility for the formation of enlarged segments in *her*-deficient embryos may be that *hairy*-related genes have been co-opted to play a role in the formation of alternate segments in vertebrates. However, we currently do not have the tools to distinguish between zebrafish vertebrae, and are therefore unable to determine if alternate segments are missing in *her1+7* MO-injected embryos.

In Meinhardt's model of somite formation, he proposes that boundaries form at the juxtaposition of anterior and posterior cell states, recognizing that an additional mechanism must operate to prevent boundary formation in the middle of a somite. [One exception to this rule is von Ebner's fissure, which only forms in the sclerotome (Keynes and Stern, 1985), and has not been observed in zebrafish.] As one mechanism to explain the inhibition of boundary formation in the middle of a somite, Meinhardt proposed the existence of a third cell state such that boundaries form between but not within somites. It has been shown in zebrafish that two cell states, anterior and posterior, are sufficient for boundary formation (Henry et al., 2000). The authors proposed that apical-basal polarity superimposed upon AP identify may specify where a boundary forms (Henry et al., 2000; Henry et al., 2001). However, in light of the 'alternate segments strengthened' phenotype of *her1+7*-deficient embryos, it is worth noting that Meinhardt also proposed that an odd-even mechanism superimposed upon AP identity could specify where a boundary forms. Clearly, *her* genes are necessary for the strengthening, on average, of every other boundary in zebrafish. Whether this 'alternate segments strengthened' phenotype reflects any conservation of segmentation between insects and vertebrates or merely reflects a crucial role for *her* genes in the segmentation clock requires further analysis.

Note added in proof

A recent paper (Holley et al., 2002) has reported that *deltaD* expression does not oscillate in zebrafish PSM. In addition, they report molecular expression analyses of *her1* MO-injected embryos similar to those reported in this paper (although we observed differences in morphological phenotype).

We thank Elizabeth Pickett and Ramona Pufan (University of California, Berkeley) and the University of Oregon Zebrafish Facility staff for excellent zebrafish care. Jennifer Anderson and Eric Parkhill provided expert technical assistance. We gratefully acknowledge our many collegues at the University of Oregon who participated in mutagenesis screening. We thank Yi-Lin Yan and John Postlethwait for generously sharing the *titin* plasmid prior to publication and Jose Campos-Ortega and Diethard Tautz for sharing information and reagents. We thank all members of the laboratory, especially Jennifer Anderson and Tina Han, for helpful discussion. This work was supported by an NIH grant (HD22486) to C. B. K. M. K. U. was supported by a National Science Foundation Predoctoral Fellowship and C. A. H. is a Miller Fellow in the Department of Molecular and Cell Biology at the University of California, Berkeley.

REFERENCES

Aulehla, A. and Johnson, R. L. (1999). Dynamic expressin of *lunatic fringe* suggests a link between *notch* signaling and an autonomous cellular oscillator driving somite segmentation. *Dev. Biol.* **207**, 49-61.

Bessho, Y., Miyoshi, G., Sakata, R. and Kageyama, R. (2001a). *Hes7*: a bHLH-type repressor gene regulated by Notch and expressed in the presomitic mesoderm. *Genes Cells* **6**, 175-185.

Bessho, Y., Sakata, R., Komatsu, S., Shiota, K., Yamada, S. and Kageyama, R. (2001b). Dynamic expression and essential functions of *Hes7* in somite segmentation. *Genes Dev.* **15**, 2642-2647.

Conlon, R. A., Reaume, A. G. and Rossant, J. (1995). *Notch1* is required for the coordinate segmentation of somites. *Development* **121**, 1533-1545.

Cooke, J. and Zeeman, E. C. (1976). A clock and wavefront model for control of the number of repeated structures during animal morphogenesis. *J. Theor. Biol.* **58**, 455-476.

Crow, M. T. and Stockdale, F. E. (1986). Myosin expression and specialization among the earliest muscle fibers of the developing avian limb. *Dev. Biol.* **113**, 238-254.

Davis, G. K. and Patel, N. H. (1999). The origin and evolution of segmentation. *Trends Cell Biol.* **104**, 868-873.

Davis, G. K. and Patel, N. H. (2002). SHORT, LONG, and BEYOND: molecular and embryological approaches to insect segmentation. *Annu. Rev. Entomol.* **47**, 669-699.

Davis, R. L. and Turner, D. L. (2001). Vertebrate hairy and Enhancer of split related proteins: transcriptional repressors regulating cellular differentiation and embryonic patterning. *Oncogene* **20**, 8342-8357.

Devoto, S. H., Melançon, E., Eisen, J. S. and Westerfield, M. (1996). Identification of separate slow and fast muscle precursor cells in vivo, prior to somite formation. *Development* **54**, 313-317.

Dubrulle, J., McGrew, M. and Pourquie, O. (2001). FGF signaling controls somite boundary position and regulates segmentation clock control of spatiotemporal *Hox* gene activation. *Cell* **106**, 219-232.

Durbin, L., Brennan, C., Shiomi, K., Cooke, J., Barrios, A., Shanmugalingam, S., Guthrie, B., Lindberg, R. and Holder, N. (1998). Eph signaling is required for segementation and differentiation of the somites. *Genes. Dev.* **12**, 3096-3109.

Durbin, L., Sordino, P., Barrios, A., Gering, M., Thisse, C., Thisse, B., Brennan, C., Green, A., Wilson, S. and Holder, N. (2000). Anteroposterior patterning is required within segments for somite boundary formation in zebrafish. *Development* **127**, 1703-1713.

Evrard, Y. A., Lun, Y., Aulehla, A., Gan, L. and Johnson, R. L. (1998). *lunatic fringe* is an essential mediator of somite segementation and patterning. *Nature* **394**, 37-81.

Forsberg, H., Crozet, F. and Brown, N. A. (1998). Waves of mouse *Lunatic fringe* expression, in four-hour cycles at two-hour intervals, precede somite boundary formation. *Curr. Biol.* **8**, 1027-1030.

Gray, M., Moens, C. B., Amacher, S. L., Eisen, J. S. and Beattie, C. E. (2001). Zebrafish *deadly seven* functions in neurogenesis. *Dev. Biol.* **237**, 306-323.

Griffin, K. J., Amacher, S. L., Kimmel, C. B. and Kimelman, D. (1998). Molecular identification of *spadetail*: regulation of zebrafish trunk and tail mesoderm formation by T-box genes. *Development* **125**, 3379-3388.

Henry, C. A., Hall, L. A., Hille, M. B., Solnica-Krezel, L. and Cooper, M. S. (2000). Somites in zebrafish doubly mutant for *knypek* and *trilobite* form without internal mesenchymal cells or compaction. *Curr. Biol.* **10**, 1063-1066.

Henry, C. A., Crawford, B. D., Yan, Y., Postlethwait, J., Cooper, M. S. and Hille, M. B. (2001). Roles for zebrafish focal adhesion kinase in notochord and somite morphogenesis. *Dev. Biol.* **240**, 474-487.

Hirsinger, E., Jouve, C., Dubrulle, J. and Pourquie, O. (2000). Somite formation and patterning. *Int. Rev. Cytol.* **198**, 1-65.

Holley, S. A., Geisler, R. and Nüsslein-Volhard, C. (2000). Control of *her1* expression during zebrafish somitogenesis by a *Delta*-dependent oscillator and an independent wave-front activity. *Genes Dev.* **14**, 1678-1690.

Holley, S. A., Jülich, D., Rauch, G.-J., Geisler, R. and Nüsslein-Volhard, C. (2002). *her1* and the *notch* pathway function within the oscillator mechanism that regulates zebrafish somitogenesis. *Development* **129**, 1175-1183.

Hrabe De Angelis, M., McIntyre, J. and Gossler, A. (1997). Maintenance of somite border in mice requires the *Delta* homologue *Dll1*. *Nature* **386**, 717-721.

Hug, B., Walter, V. and Grunwald, D. J. (1997). *tbx6*, a *Brachyury*-related gene expressed by ventral mesendodermal precursors in the zebrafish embryo. *Dev. Biol.* **183**, 61-73.

Jen, W. C., Gawantka, V., Pollet, N., Niehrs, C. and Kintner, C. (1999).

Periodic repression of Notch pathway genes governs the segmentation of *Xenopus* embryos. *Genes Dev.* **13**, 1486-1499.

Jiang, Y. L., Aerene, B. L., Smithers, L., Haddon, C., Ish-Horowicz, D. and Lewis, J. (2000). Notch signalling and the synchronization of the somite segmentation clock. *Nature* **408**, 475-479.

Jouve, C., Palmeirim, I., Henrique, D., Beckers, J., Gossler, A., Ish-Horowicz, D. and Pourquie, O. (2000). Notch signalling is required for cyclic expression of the hairy-like gene *HES1* in the presomitic mesoderm. *Development* **127**, 142-1429.

Jowett, T. (1999). Analysis of protein and gene expression. *Methods Cell. Biol.* **59**, 63-85.

Keynes, R. J. and Stern, C. D. (1985). Segmentation and neural development. *Trends Neurosci.* **8**, 220-223.

Keynes, R. J. and Stern, C. D. (1988). Mechanisms of vertebrate segmentation. *Development* **103**, 413-429.

Kim, S., Yamamoto, A., Bouwmeester, T., Agius, E. and De Robertis, E. M. (1998). The role of Paraxial Protocadherin in selective adhesion and cell movements of the mesoderm during *Xenopus* gastrulation. *Development* **125**, 4681-4691.

Kimmel, C. B., Ballard, W. W., Kimmel, S. R., Ullmann, B. and Schilling, T. F. (1995). Stages of embryonic development of the zebrafish. *Dev. Dyn.* **203**, 253-310.

Koizumi, K., Nakajima, M., Yuasa, S., Saga, Y., Sakai, T., Kuriyama, T., Shirasawa, T. and Koseki, H. (2001). The role of presenilin 1 during somite segmentation. *Development* **128**, 1391-1402.

Krauss, S., Johansen, T., Korzh, V. and Fjose, A. (1991). Expression of the zebrafish paired box gene *pax[zf-b]* during early neurogenesis. *Development* **113**, 1193-1206.

Kusumi, K., Sun, E., Kerrebrock, A., Bronson, R., Chi, D., Bulotsky, M., Spencer, J., Birren, B., Frankel, W. and Lander, E. (1998). The mouse pudgy mutation disrupts *delta* homologue *dll3* and initiation of early somite boundaries. *Nat. Genet.* **19**, 274-278.

Leimeister, C., Dale, K., Fischer, A., Klamt, B., de Angelis, M., H., Radtke, F., McGrew, M. J., Pourquie, O. and Gessler, M. (2000). Oscillating expression of *c-Hey2* in the presomitic mesoderm suggests that the segmentation clock may use combinatorial signaling through multiple interacting bHLH factors. *Dev. Biol.* **227**, 91-103.

Maderspacher, F., Bucher, G. and Klinger, M. (1998). Pair-rule and gap gene mutants in the flour beetle *Tribolium castaneum*. *Dev. Genes Evol*. **208**, 558-568.

McGrew, M. J., Dale, J. K., Fraboulet, S. and Pourquie, O. (1998). The *lunatic fringe* gene is a target of the molecular clock linked to somite segmentation in avian embryos. *Curr. Biol*. **8**, 487-493.

Meinhardt, H. (1986). Models of segmentation. In *Somites in Developing Embryos* (ed. R. Bellairs, D. A. Edde and J. W. Lash), pp 179-191. New York/London: Plenum.

Moens, C. B., Cordes, S. P., Giorgianni, M. W., Barsh, G. S. and Kimmel, C. B. (1998). Equivalence in the genetic control of hindbrain segmentation in fish and mouse. *Development* **125**, 381-391.

Moens, C. B., Yan, Y. L., Appel, B., Force, A. G. and Kimmel, C. B. (1996). *valentino*: a zebrafish gene required for normal hindbrain segmentation. *Development* **122**, 3881-3891.

Müller, M., Weizsäcker, E. and Campos-Ortega, J. A. (1996). Expression domains of a zebrafish homologue of the *Drosophila* pair-rule *hairy* correspond to primordia of altering somites. *Development* **122**, 2017-2078.

Nasevicius, A. and Ekker, S. C. (2000). Effective target gene 'knockdown' in zebrafish. *Nature Genet.* **26**, 216-220.

Odenthal, J. and Nüsslein-Volhard, C. (1998). Fork head domain genes in zebrafish. *Dev. Genes. Evol*. **208**, 245-258.

Oka, C., Nakano, T., Wakeham, A., de la Pompa, J. L., Mori, C., Sakai, T., Okazaki, S., Kawaichi, M., Shiota, K., Mak, T. W. et al. (1995). Disruption of the mouse *RBP-J kappa* gene results in early embryonic death. *Development* **121**, 3291-3301.

Palmeirim, J., Henrique, D., Ish-Horomicz, D. and Pourquié, O. (1997). Avian *hairy* gene expression identifies a molecular clock linked to vertebrate segmentation and somitogenesis. *Cell* **91**, 639-648.

Pasini, A., Henrique, D. and Wilkinson, D. G. (2001). The zebrafish Hairy/Enhancer-of-split-related gene *her6* is segmentally expressed during the early development of hindbrain and somites. *Mech. Dev.* **100**, 317-321.

Pick, L. (1998). Segmentation: Painting Stripes From Flies to Vertebrates. *Dev. Genet.* **23**, 1-10.

Postlethwait, J. H., Johnson, S. L., Midson, C. N., Talbot, W. S., Gates, M., Ballinger, E. W., Africa, D., Andrews, R., Carl T., Eisen, J. S. et al. (1994). A genetic linkage map for the zebrafish. *Science* **264**, 699-703.

Sawada, A., Fritz, A., Jiang, Y. J., Yamamoto, A., Yamasu, K., Kuroiwa, A., Saga, Y. and Takeda, H. (2000). Zebrafish Mesp family genes, *mesp-a* and *mesp-b* are segmentally expressed in the presomitic mesoderm, and Mesp-b confers the anterior identity to the developing somites. *Development* **127**, 1691-1702.

Sawada, A., Shinya, M., Jiang, Y., Kawakami, A. and Takeda, H. (2001). Fgf/MAPK signalling is a crucial positional cue in somite boundary formation. *Development* **128**, 4873-4880.

Sprague, J., Doerry, E., Douglas, S., Westerfield, M. and ZFIN group (2001). The Zebrafish Information Network (ZFIN): a resource for genetic, genomic and developmental research. *Nucl. Acids. Res.* **29**, 87-90.

Sulston, I. A. and Anderson, K. V. (1996). Embryonic patterning mutants of *Tribolium castaneum*. *Development* **122**, 805-814.

Sulston, I. A. and Anderson, K. V. (1998). Altered patterns of gene expression in *Tribolium* segmentation mutants. *Dev. Genet.* **23**, 56-64.

Takahashi, Y., Koizumi, K., Takagi, A., Kitajima, S., Inoue, T., Koseki, H. and Saga, Y. (2000). Mesp2 initiates somite segmentation through the Notch signalling pathway. *Nat. Genet.* **25**, 174-189.

Takebayashi, K., Sasai, Y., Sakai, Y., Watanabe, T., Nakanishi, S. and Kageyama, R. (1994). Structure, chromosomal locus, and promoter analysis of the gene encoding the mouse helix-loop-helix factor HES-1. Negative autoregulation through the multiple N box elements. *J. Biol. Chem.* **7**, 5150-5156.

Takke, C. and Campos-Ortega, J. A. (1999). *her1*, a zebrafish pair-rule like gene, acts downstream of notch signalling to control somite development. *Development* **126**, 3005-3014.

Takke, C., Dornseifer, P., von Weizsacker, E. and Campos-Ortega, J. A. (1999). *her4*, a zebrafish homologue of the *Drosophila* neurogenic gene *E(spl)*, is a target of NOTCH signalling. *Development* **126**, 1811-1821.

Talbot, W. S., Trevarrow, B., Halpern, M. E., Melby, A. E., Farr, G., Postlethwait, J. H., Jowett, T., Kimmel, C. B. and Kimelman, D. (1995). A homeobox gene essential for zebrafish notochord development. *Nature* **378**, 150-157.

Thisse, C., Thisse, B., Halpern, M. E. and Postlethwait, J. H. (1994). *goosecoid* expression in neurectoderm and mesendoderm is disrupted in zebrafish *cyclops* gastrulas. *Dev. Biol.* **164**, 420-429.

Topczewska, J. M., Topczewski, J., Shostak, A., Kume, T., Solnica-Krezel, L. and Hogan, B. L. M. (2001). The winged helix transcription factor Foxc1a is essential for somitogenesis in zebrafish. *Genes Dev.* **15**, 2483-2493.

van Eeden, F. J., Granato, M., Schach, U., Brand, M., Furutni-Seki, M., Haffter, P., Hammerschmidt, M., Heisenberg, C. P., Jiang, Y. J., Kane, D. A. et al. (1996). Mutations affecting somite formation and patterning in the zebrafish, *Danio rerio*. *Development* **123**, 153-164.

van Eeden, F. J., Holley, S.A., Haffter, P. and Nüsslein-Volhard, C. (1998). Zebrafish segmentation and pair-rule patterning. *Dev. Genet.* **23**, 65-76.

Walker, C. (1999). Haploid screens and γ-ray mutagenesis. *Methods Cell. Biol.* **60**, 43-70.

Weinberg, E. S., Allende, M. L., Kelly, C. S., Abdelhamid, A., Murakami, T., Andermann, P., Doerre, O. G., Grunwald, D. J. and Riggleman, B. (1996). Developmental regulation of zebrafish *MyoD* in wild-type, *no tail* and *spadetail* embryos. *Development* **122**, 271-280.

Westerfield, M. (1995). *The Zebrafish Book: a guide for the laboratory use of zebrafish* (Danio rerio), 3rd edition. Oregon: University of Oregon Press.

Wettstein, D. A., Turner, D. L. and Kintner, C. (1997). The *Xenopus* homolog of *Drosophila* Suppressor of Hairless mediates Notch signaling during primary neurogenesis. *Development* **124**, 693-702.

Wood, A. and Thorogood, P. (1994). Patterns of cell behaviour underlying somitogenesis and notochord formation in intact vertebrate embryos. *Dev. Dyn.* **201**, 151-167.

Yamamoto, A., Amacher, S. L., Kim, S. H., Geissert, D., Kimmel, C. B. and De Robertis, E. M. (1998). Zebrafish *paraxial protocadherin* is a downstream target of *spadetail* involved in morphogenesis of gastrula mesoderm. *Development* **125**, 3389-3397.

Yan, Y.-L., Singer, A., Miller, C., Nissen, R., Liu, D., Kirt, A., Draper, B., Willoughby, J., Marcos, P., Chung, B.-C., Haffter, P., Westerfield, M., Hopkins, N., Kimmel, C. and Postlethwait, J. H. (2002). Activity of a *sox9* gene is required for stacking of chondrocytes in cartilage development. *Development* in press.

Zhang, N. and Gridley, T. (1998). Defect in somite formation in *lunatic fringe*-deficient mice. *Nature* **394**, 374-377.